PHOTONIC SENSORS / Vol. 10, No. 2, 2020: 162–170

Enhanced Plasmonic-Induced Absorption Using a Cascade Scheme and Its Application as Refractive-Index Sensor

Xinyi LI[1], Daobin WANG[2*], Shoupeng WANG[2], Lihua YUAN[2], Jingli LEI[2], and Xiaoxiao LI[2]

[1]*School of Architecture & Urban Planning, Lanzhou Jiaotong University, Lanzhou 730070, China*

[2]*School of Science, Lanzhou University of Technology, Lanzhou 730050, China*

[*]Corresponding author: Daobin WANG E-mail: photonics_wang@yahoo.com

Abstract: In this paper, we describe a new method to improve fast-light transmission, which uses cascades. We design a simple plasmonic device that enables plasmonic-induced absorption (PIA). It consists mainly of two parallel rectangular cavities. The numerical results simulated by using the finite element method (FEM) confirm its function. The corresponding group delay-time can reach –0.146 ps for the PIA window. Based on this result, we propose a cascade device, with the dual-rectangular cavity system as building block, to improve fast-light transmission even more. The results indicate that the cascade scheme can increase the group delay-time to –0.456 ps, which means the fast-light feature is substantially enhanced compared with the non-cascading approach. The effect of the distance between two cascade resonators and other structural parameters is also investigated. Finally, we use this design concept to build a refractive-index sensor with a sensitivity of 701 nm/RIU.

Keywords: Plasmonic-induced absorption; fast light; metal-insulator-metal waveguide; finite element method

Citation: Xinyi LI, Daobin WANG, Shoupeng WANG, Lihua YUAN, Jingli LEI, and Xiaoxiao LI, "Enhanced Plasmonic-Induced Absorption Using a Cascade Scheme and Its Application as Refractive-Index Sensor," *Photonic Sensors*, 2020, 10(2): 162–170.

1. Introduction

Electromagnetically induced absorption (EIA) appeared first as a quantum mechanical phenomenon in atomic media, where the absorption of a laser beam increased significantly but only for a narrow frequency band [1, 2]. Within the narrow frequency band (the absorption window), anomalous dispersion can be created, which leads to superluminal propagation, i.e., "fast light" [3]. Unfortunately, atomic EIA often requires very specific operating conditions including stable gas-lasers and a low-temperature environment, which makes many applications problematic. In recent years, it was found that the EIA effects can also be realized in classical configurations such as coupled dielectric resonators, acoustic waveguides, planar metamaterials, and plasmonic nanodevices [4]. More specifically, plasmonic-induced absorption (PIA) in metal-insulator-metal (MIM) waveguides [5–12] has attracted a lot of interest. For example, PIA was observed in a plasmonic coupling system consisting of MIM bus waveguides and two concentric nano-rings [5]. In [6], a simple MIM plasmonic device, consisting of two rectangle cavities, was designed and

Received: 22 January 2019 / Revised: 8 April 2019

DOI: 10.1007/s13320-019-0561-x
Article type: Regular

investigated. Moreover, the perfect PIA effect with fast-light performance was observed in this device. The authors of [7] proposed an end-coupled composite-slot-cavity resonator using MIM waveguides. The PIA response in this device was studied and confirmed by using the coupled-mode theory [13] and the finite-difference time-domain (FDTD) method [14].

In this paper, we first design a simple plasmonic device on a nanoscale. It consists of a dual-rectangular cavity system coupled to MIM bus waveguides. Numerical simulations using the finite element method (FEM) were carried out to investigate the transmission spectra and field distribution. The results show that the PIA effect can indeed be observed. Furthermore, by changing the structural parameters, the fast-light characteristics of this plasmonic system can be adjusted. We then describe a cascade-based scheme to improve the fast-light performance for PIA. While the cascade-based method has been used previously to enhance plasmonic-induced transparency (PIT) [15], to the best of our knowledge, no studies exist that focus on the cascade-based method in association with PIA. Our results confirm the feasibility of this approach. This study opens a new door for the development of ultracompact high-performance fast-light devices in high-speed optical communication networks [16, 17].

2. Device design

The proposed cascading device for fast-light transmission uses a dual-rectangular cavity system as its building block. Every dual-rectangular cavity system is represented by a meta-atom. Two meta-atoms are placed in a cascade to enhance fast-light performance, as shown in Fig. 1. Each meta-atom, surrounded by a blue dashed line in Fig. 1, consists of two MIM waveguides, a fixed rectangular cavity (FRC), and an adjustable rectangular cavity (ARC). The fixed rectangular cavity is placed between the input and output MIM waveguides with a coupling distance g_1. The adjustable rectangular cavity is placed next to the fixed rectangular cavity to generate the PIA response. Here, g_2 is the coupling distance between the fixed and the adjustable rectangular cavities. To ensure fundamental transverse-magnetic (TM_0) mode propagation in the MIM waveguide, the widths of the MIM waveguides, fixed rectangular cavity, and adjustable rectangular cavity are fixed at 50 nm, i.e., W_g=W_{frc}=W_{arc}=50 nm. L_{frc} and L_{arc} are the lengths of the fixed and adjustable rectangular cavities, respectively. The white area in Fig. 1 represents the air in the waveguides and cavities. When this device is used as a refractive-index sensor, the liquid analytes with refractive indices of about 1.33 are filled into FRC and ARC. The gray area represents silver, which has a frequency-dependent complex relative permittivity as described by the Drude model [18]:

$$\varepsilon(\omega)=\varepsilon_{\infty}-\frac{\omega_p^2}{\omega(\omega+\mathrm{i}\gamma)} \tag{1}$$

where ε_{∞}=3.7 represents the dielectric constant at the infinite frequency, γ=2.73×10^{13} Hz is the electron collision frequency, ω_p =1.38×10^{16} Hz is the bulk plasma frequency, and ω stands for the angular frequency of the incident light.

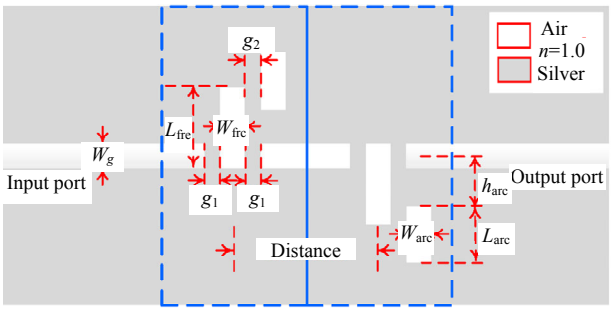

Fig. 1 Proposed cascade scheme using a dual-rectangular cavity system as building block.

3. Results and discussion

3.1 Non-cascading Device

To assess the performance of a single meta-atom, the transmission (T), reflection (R), and absorption

(A) spectra were investigated by using FEM with a perfectly matched layer (PML) boundary condition. R and T are calculated by using the scattering matrix elements of the device:

$$R=\left|S_{11}\right|^2,\ T=\left|S_{21}\right|^2. \tag{2}$$

Here, absorption can be deduced using A=1−R−T. The obtained results for L_{frc}=L_{arc}=200 nm and g_1=g_2=15 nm are shown in Fig. 2. For a clear comparison, the transmission spectrum of the device without an adjustable rectangular cavity is also marked, as shown by the gray-dashed line in Fig. 2. A distinct PIA window appears around the transmission peak of the device without an adjustable rectangular cavity. In addition, two new transmission peaks with incident wavelengths of 659.91 nm and 733.18 nm appear around the PIA window. The insets of Fig. 2 show the field distribution of H_z at the wavelengths of 659.91 nm, 674.92 nm, and 733.18 nm, respectively. Based on these results, we can infer that the reason for PIA is the destructive interference in the fixed rectangular cavity. There are two propagation paths for the optical signal in this device. The first path is the direct coupling of optical signals between the fixed rectangular cavity and the input/output MIM waveguides. The second path is the indirect coupling of optical signals that occurs between the adjustable rectangular cavity and the input/output waveguides. The fixed rectangular cavity acts as intermediary. Consequently, the destructive interference between these two pathways suppresses the fixed rectangular cavity. However, the adjustable rectangular cavity can still be activated efficiently, which causes very low transmittance at λ=674.92 nm, and the PIA effect is successfully generated in our proposed device. Two new peaks appear in the transmission spectrum, which can be attributed to in-phase coupling and out-of-phase coupling between the fixed and adjustable rectangular cavities. The in-phase coupling resonance results in the peak at λ=659.91 nm, whereas the out-of-phase coupling resonance produces the peak at λ=733.18 nm.

The fast-light performance of the MIM devices is usually characterized by an abnormal dispersion and group delay time. The group delay time is defined by the following equation: $t_g=d\Phi(\omega)/d\omega$ [19, 20], where $\Phi(\omega)$ is the transmitted phase of the right MIM waveguide.

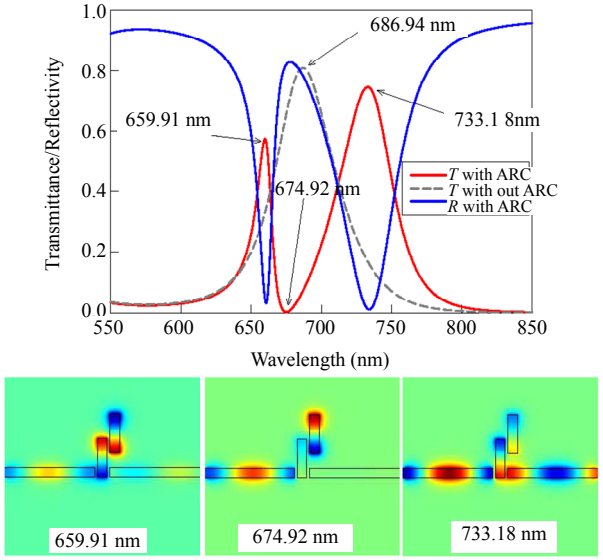

Fig. 2 Transmission and absorption spectra of the dual-rectangular cavity system, the insets show the field distribution of H_z at the wavelength of 659.91 nm, 674.92 nm and 733.18 nm, respectively.

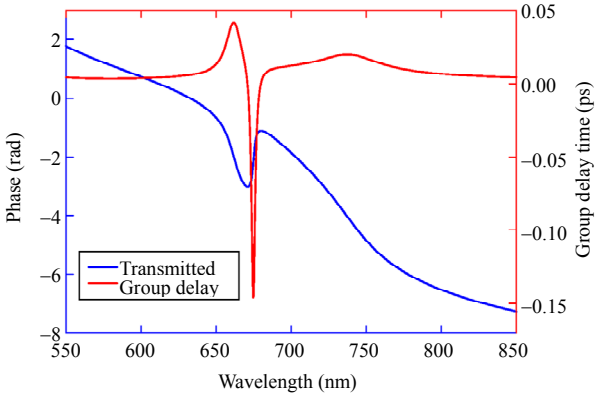

Fig. 3 Variations of the transmitted phase and the group delay time with respect to the wavelength of incident light.

Figure 3 shows the variations of the transmitted phase and the group delay-time with respect to the wavelength. A distinct π phase-shift occurs at the PIA window in the proposed device. Considering the relationship (derivative) between the transmitted phase and the group delay-time, it can be concluded

that abnormal dispersion occurs for the PIA window. As illustrated in Fig. 3 with the red-solid line, a group delay-time of up to –0.146 ps was observed for the central wavelength of the PIA window. Thanks to this unique property, one can easily manipulate the on-chip fast-light transmission with this subwavelength MIM waveguide device.

3.2 Cascade device

In this section, we investigate the cascade device. Two meta-atoms were arranged in a cascade to improve fast-light performance, as shown in Fig. 1. To achieve this goal, we set L_{frc}=L_{arc}=200 nm and g_1=g_2=15 nm. The distance between two meta-atoms was 200 nm. Figure 4(a) shows the transmission spectrum for the cascade device. For comparison, the transmission spectrum of the non-cascading device is also shown. Due to the introduction of an extra meta-atom, the maximum transmittance of our proposed MIM device is slightly reduced. The fast-light performance of the proposed cascade device is shown in Fig. 4(d). Using this figure, a group delay-time of up to –0.3014 ps can be obtained with the cascade device. It is very clear that, by combining up two meta-atoms as depicted in Fig. 1, the fast-light performance of the proposed plasmonic device can be substantially improved and adjusted.

As a result, we investigate if it is possible to control the fast-light performance by using subtle structural modifications. One factor that affects the fast-light performance is the distance between the cascade resonators. Figures 5(a)–5(e) show the transmission spectra for different distances. Figure 5(f) shows the corresponding maximum modulus of t_g. According to the calculation, the distance between two meta-atoms increases from 100 nm to 200 nm, with 25 nm increments. Using these results, we find that the maximum transmittance decreases with the distance, while the corresponding resonant wavelength of the PIA window shows a slight red shift when the distance increases. In this paper, we limit the distance between 100 nm and 200 nm. In fact, the dielectric spacer in the center would disappear if the distance between the cascade resonators was below 80 nm. Considering the already obtained results, the fast-light performance of the proposed device would be seriously degraded in this case. When the distance between the cascade resonators is too large,

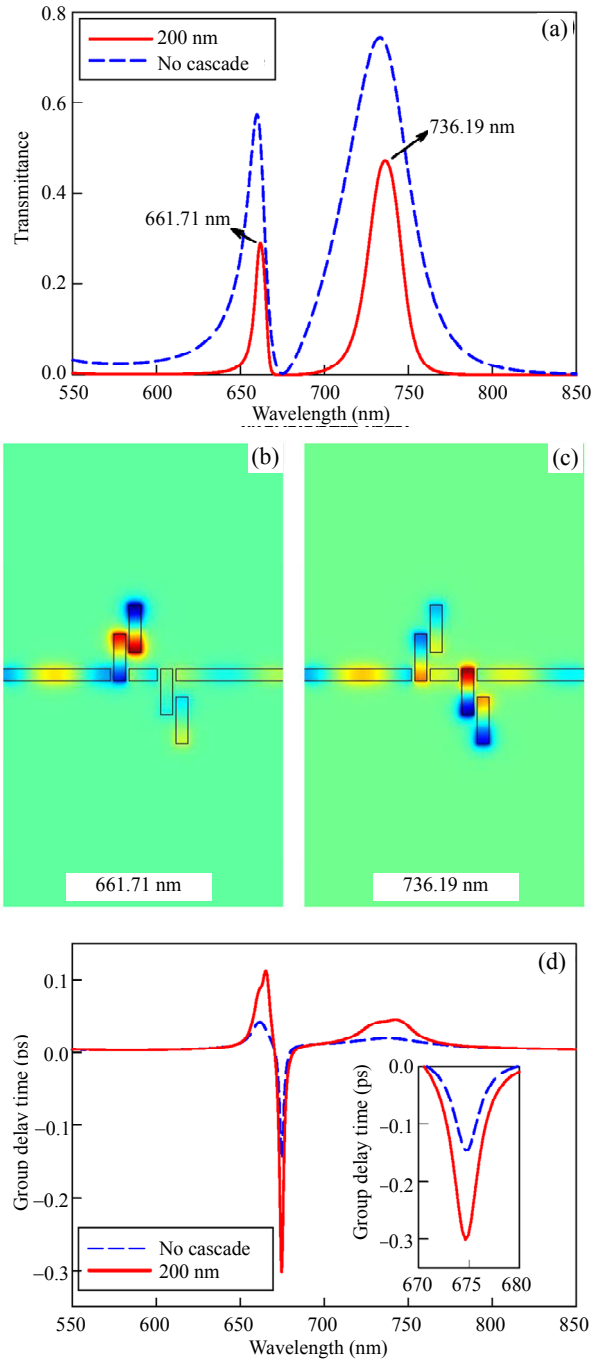

Fig. 4 Transmission spectrum (a) and group delay time (d) of the proposed cascade device. For convenience, corresponding results of the non-cascading device are also shown using blue-dashed line in these figures. (b), (c) Corresponding magnetic field distributions for the two resonance peaks.

the dielectric spacer in the center induces Fabry-Pérot resonance. In the following, if not otherwise stated, the distance between the cascade resonators was fixed at 200 nm.

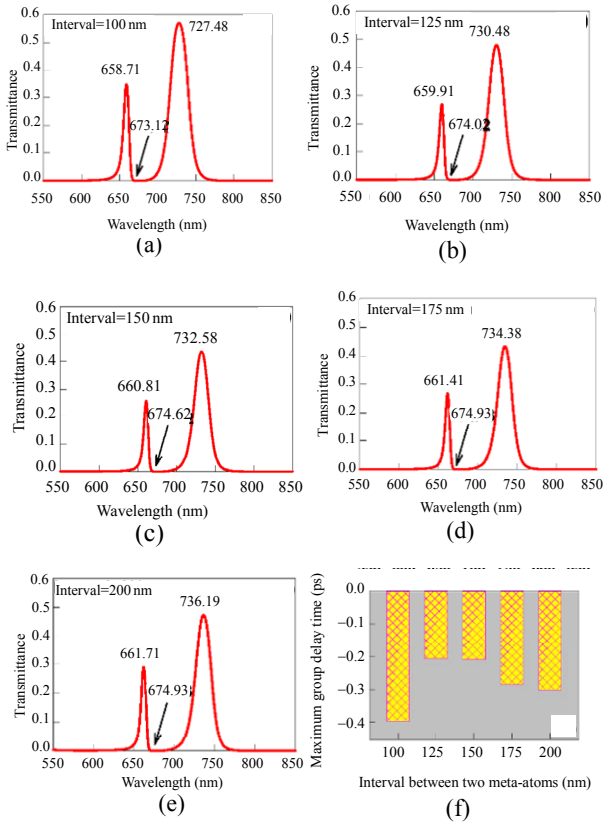

Fig. 5 Transmission spectra (a)–(e) and the maximum group delay time (f) of the cascade device for different distances.

Another important factor affecting the fast-light performance is the length of the adjustable rectangular cavities. The variations of the group delay-time with respect to L_{arc} are shown in Figs. 6(a) and 6(b) for a single resonator and a cascade device. For the calculation of these results, the central position of the adjustable rectangular cavity is fixed and L_{arc} varies between 170 nm and 210 nm with an increment of 10 nm. Apart from the apparent red-shift of the PIA window, it can be also found that the maximum modulus of t_g increases with the length L_{arc}. This reinforcing effect is particularly strong in the cascade device. According to Fig. 6(b), the group delay-time at the center wavelength of the PIA window could be further enhanced to –0.314 ps, when L_{arc}=210 nm. For a single resonator, the enhancement of L_{arc} with respect to the fast-light performance still exists. However, the increase is much smaller than that for the cascade device. The fast-light performance of our proposed device, however, cannot be infinitely enhanced by modifying L_{arc}. When L_{arc} is too high, the adjustable rectangular cavities start coupling to the dielectric spacer in the center and other parts of this device. These interactions can reduce the fast-light performance of this cascade device.

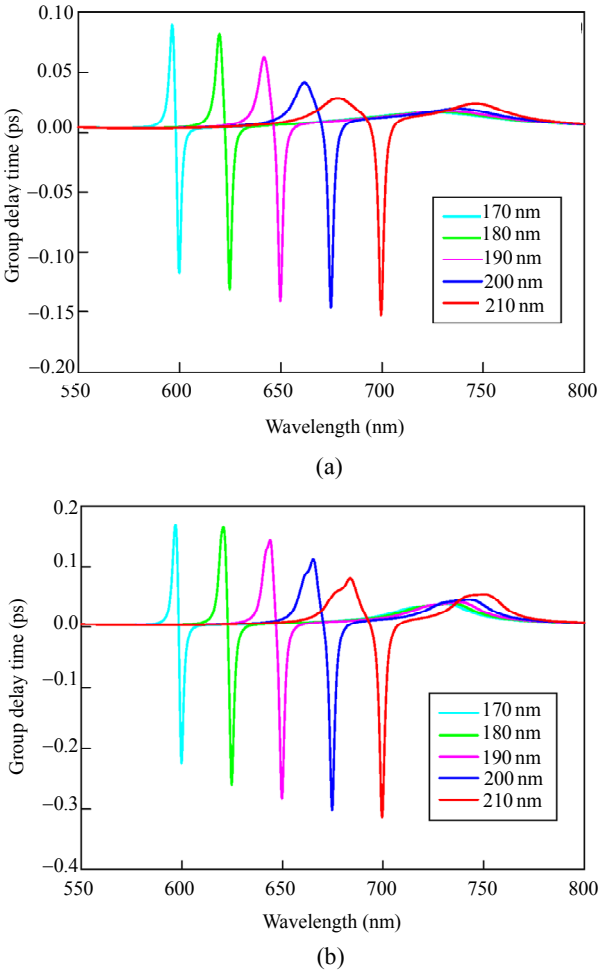

Fig. 6 Group delay time versus L_{arc} for (a) the non-cascading device and (b) cascade device.

Until now, two meta-atoms were cascaded to form a single-period pattern. From now on, we investigate whether the fast-light performance can be improved by adding more periods to the cascade resonators. For this purpose, three meta-atoms were

cascaded to produce a two-period pattern. The transmission and absorption spectra for the two-period pattern are shown in Fig. 7(a). To enable a better comparison, the results for the single-period patterns are also shown. Figures 7(b) and 7(c) show the field distribution by H_z at the transmission peaks. The corresponding group delay-times are plotted in Fig. 7(d). To obtain these results, we set L_{arc}=200 nm and g_1=g_2=15 nm. These results indicate that the maximum transmittance could decrease further if more periods of the cascade resonators were added. However, we also found that the maximum modulus of t_g increases to –0.456 ps under this condition, which means that the fast-light performance of our proposed device is improved. We also study the fast-light performance of three-period pattern which is produced by cascading four meta-atoms together. Obtained results show that the maximum modulus of t_g is further increased to –0.618 ps, while the maximum transmittance is reduced to a very small value. All results show that the cascade method can effectively realize plasmonic-induced absorption and improve fast-light transmission. As we can see from above results, the propagation loss is the obstacle that hinders the practical application of the cascade scheme. The more meta-atoms are cascaded, the larger propagation loss conspicuously becomes. One possible solution is to introduce the gain material [21] or nonlinear material [22, 23] into the cascade device. We can replace the passive dielectric part of the cascade device with gain material to compensate for propagation loss. This topic is beyond the scope of this paper and needs further investigation in the future.

3.3 Ultra-compact refractive index sensor

The PIA effect can be used for many different scenarios including ultrafast optical switching in photonic integrated devices [24] and fast-light applications [25]. One very important application is a high-performance sensor [26]. In this paper, we propose a new design of a refractive-index sensor, which uses cascaded plasmonic resonators. We use the single-period device and fill liquid analytes with refractive indices of about 1.33 in FRC and ARC. The liquid analytes can be filled into FRC and ARC

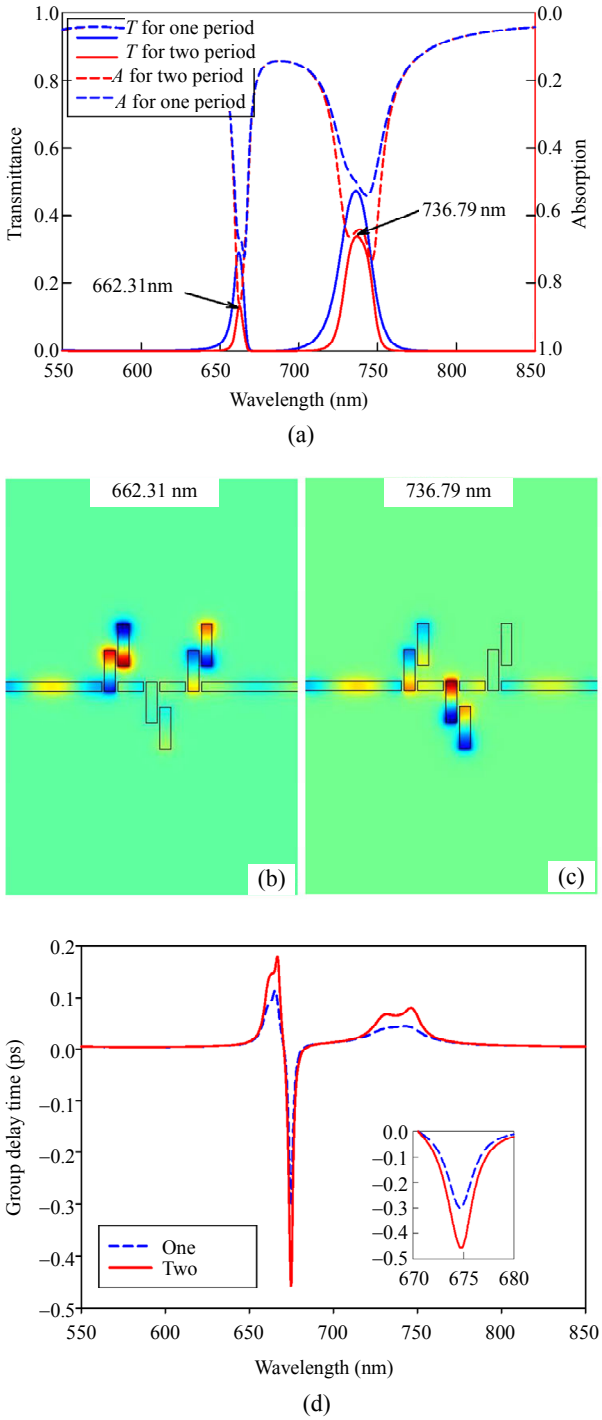

Fig. 7 Tansmission/absorption spectra: (a) and group delay time, (d) of the proposed device with one period (blue line) and two period (red line), and (b)–(c) H_z field distribution corresponding to the wavelengths of 662.31 and 736.79 nm.

via standard microfluidic pumps or via capillary forces [27]. Here, L_{frc}=200 nm and L_{arc}=210 nm. Figure 8(a) shows the effect of the analyte refractive index on the transmission spectrum of this sensor. A substantial red-shift is achieved for the resonance peak wavelengths, when the analyte refractive index increases. The resonance peak wavelength as a function of the analyte refractive index change is shown in Fig. 8 (b). The refractive index sensitivity of this sensor is 634 nm/RIU and 701 nm/RIU for the resonance peaks, Peak I and Peak II, respectively.

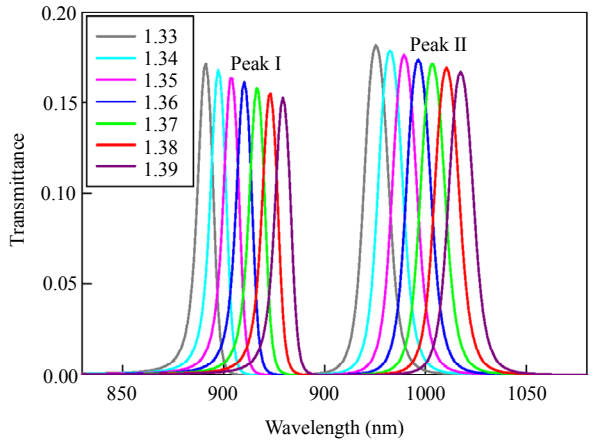

(a)

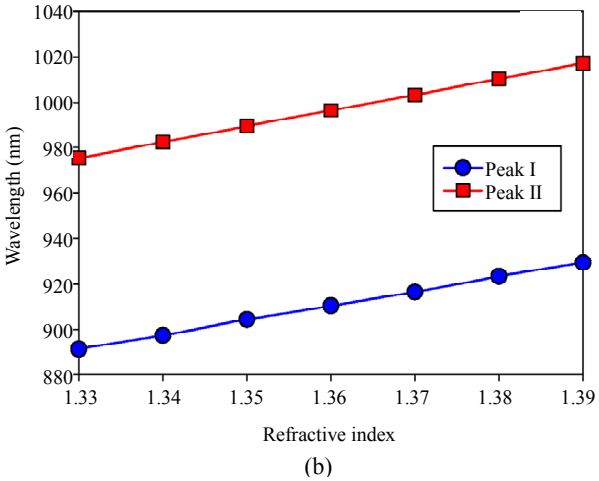

(b)

Fig. 8 Refractive index sensing performance of our proposed device: (a) transmission spectra of the proposed device for different refractive indices of the liquid analytes filled in FRC and ARC and (b) the resonance peak wavelengths versus analyte refractive index change for L_{arc}=210 nm.

In Table 1, the fast-light performance and sensitivity of different devices are compared with those of our proposed device. One can see that our proposed device can provide a large group delay time of –0.456 ps when three meta-atoms are cascaded to produce a two-period pattern. The refractive-index sensor based on the proposed device has a comparable sensitivity with that in [26]. The devices in [24] and [30] exhibit very high sensitivity. However, the excellent sensing performance is usually achieved at the expense of the large sensor size. The plasmonic cavity length in [24] is about 1020 nm which is much larger than ours (210 nm). Our results demonstrate that the PIA effect has a great potential for applications in plasmonic sensors.

Table 1 Comparison of the proposed device and other published solutions.

Reference	Group delay time (ps)	Sensitivity (m/RIU)
[5]	–0.098	NA
[20]	–0.29	NA
[7]	–0.30	NA
[28]	–0.40	NA
[29]	–0.25	615
[26]	NA	859
[30]	NA	1150
[24]	NA	2025
This work	–0.456	701

4. Conclusions

In summary, we introduce and investigate a cascading nanodevice to enable fast-light transmission by using a dual-rectangular cavity system as building block. Numerical simulations using FEM are carried out to investigate the transmission spectra and field distribution. We find that the fast-light transmission using cascades is significantly higher than that without cascades. The effect of important parameters on the fast-light performance, such as period and cavity length, is studied and a refractive-index sensor is designed based on the proposed device. The device has a refractive-index sensitivity of 701 nm/RIU. This study opens a new door for the development of ultracompact high-performance fast-light devices.

Acknowledgment

This work was supported by the National Natural Science Foundation of China (Grant No.

61367007), the Natural Science Fund of Gansu Province of China (Grant Nos. 17JR5RA123 and 17JR5RA132), and the HongLiu First-Class disciplines Development Program of Lanzhou University of Technology.

References

[1] A. M. Akulshin, S. Barreiro, and A. Lezama, "Steep anomalous dispersion in coherently prepared Rb vapor," *Physical Review Letters*, 1999, 83(21): 4277–4280.

[2] H. Failache, P. Valente, G. Ban, V. Lorent, and A. Lezama, "Inhibition of electromagnetically induced absorption due to excited-state decoherence in Rb vapor," *Physical Review A*, 2003, 67(4): 043810.

[3] C. P. Liu, S. Q. Gong, X. J. Fan, and Z. Z. Xu, "Electromagnetically induced absorption via spontaneously generated coherence of a system," *Optics Communications*, 2004, 231(1): 289–295.

[4] M. Fleischhauer, A. Imamoglu, and J. P. Marangos, "Electromagnetically induced transparency: optics in coherent media," *Reviews of Modern Physics*, 2005, 77(2): 633–673.

[5] H. J. Li, L. L. Wang, and X. Zhai, "Plasmonically induced absorption and transparency based on MIM waveguides with concentric nanorings," *IEEE Photonics Technology Letters*, 2016, 28(13): 1454–1457.

[6] S. L. Yang, D. M. Yu, G. D. Liu, Q. Lin, X. Zhai, and L. L. Wang, "Perfect plasmon-induced absorption and its application for multi-switching in simple plasmonic system," *Plasmonics*, 2018, 13(3): 1015–1020.

[7] K. Wen, Y. Hu, J. Zhou, L. Lei, J. Li, and Y. Wu, "Plasmonic-induced absorption in an end-coupled metal-insulator-metal resonator structure," *Optical Materials Express*, 2017, 7(2): 433–443.

[8] P. Tassin, L. Zhang, R. Zhao, A. Jain, T. Koschny, and C. M. Soukoulis, "Electromagnetically induced transparency and absorption in metamaterials: the radiating two-oscillator model and its experimental confirmation," *Physical Review Letters*, 2012, 109(18): 187401.

[9] R. Taubert, M. Hentschel, J. Kastel, and H. Giessen, "Classical analog of electromagnetically induced absorption in plasmonics," *Nano Letters*, 2012, 12(3): 1367–1371.

[10] A. Mahigir, P. Dastmalchi, W. Shin, S. Fan, and G. Veronis, "Plasmonic coaxial waveguide-cavity devices," *Optics Express*, 2015, 23(16): 20549–20562.

[11] X. Zhang, N. Xu, K. Qu, Z. Tian, R. Singh, J. Han, *et al.*, "Electromagnetically induced absorption in a three-resonator metasurface system," *Scientific Report*, 2015, 5: 10737.

[12] J. Wang, F. Zhang, Y. Pan, J. Lu, and X. Ni, "Tunable plasmonic band-pass filter with dual side-coupled circular ring resonators," *Sensors*, 2017, 17(3): 585–593.

[13] Q. Li, T. Wang, Y. Su, M. Yan, and M. Qiu, "Coupled mode theory analysis of mode-splitting in coupled cavity system," *Optics Express*, 2010, 18(8): 8367–8382.

[14] A. Taflove and S. Hagness, Computational electromagnetics: the finite-difference time-domain method (3rd ed). Norwood, MA, USA: Artech House, 2005.

[15] S. Zhan, H. Li, G. Cao, Z. He, B. Li, and H. Yang, "Slow light based on plasmon-induced transparency in dual-ring resonator-coupled MDM waveguide system," *Journal of Physics D: Applied Physics*, 2014, 47(20): 205101.

[16] Y. Zhao, B. Chen, J. Zhang, and X. Wang, "Energy efficiency with sliceable multi-flow transponders and elastic regenerators in survivable virtual optical networks," *IEEE Transactions on Communications*, 2016, 64(6): 2539–2550.

[17] Y. Zhao, R. He, H. Chen, J. Zhang, Y. Ji, H. Zheng, *et al.*, "Experimental performance evaluation of software defined networking (SDN) based data communication networks for large scale flexi-grid optical networks," *Optics Express*, 2014, 22(8): 9538–9547.

[18] Z. Han and S. I. Bozhevolnyi, "Plasmon-induced transparency with detuned ultracompact Fabry-Perot resonators in integrated plasmonic devices," *Optics Express*, 2011, 19(4): 3251–3257.

[19] X. Zhang, H. Y. Meng, S. Liu, X. C. Ren, C. H. Tan, Z. C. Wei, *et al.*, "Plasmonically induced absorption and transparency based on stub waveguide with nanodisk and Fabry-Perot resonator," *Plasmonics*, 2017, 12(5): 1289–1296.

[20] K. Wen, Y. Hu, L. Chen, J. Zhou, M. He, L. Lei, *et al.*, "Plasmonic-induced absorption and transparency based on a compact ring-groove joint MIM waveguide structure," *IEEE Photonics Journal*, 2016, 8(5): 1–8.

[21] N. Liu, H. Wei, J. Li, Z. X. Wang, X. R. Tian, A. L. Pan, *et al.*, "Plasmonic amplification with ultra-high

optical gain at room temperature," *Scientific Reports*, 2013, 3: 1967.

[22] B. Liu, Y. C. Liao, J. F. Hu, J. Liu, X. D. He, and Z. P. Chen, "Plasmon-induced reflection and its application for all-optical diode based on paralleled double-stub resonators," *Applied Physics Express*, 2019, 12(3): 032011.

[23] H. Q. Liang, B. Liu, J. F. Hu, and X. D. He, "High efficiency all-optical plasmonic diode based on a nonlinear side-coupled waveguide-cavity structure with broken symmetry," *Optics Communications*, 2018, 414: 98–101.

[24] S. Yadollah and V. Mohammad, "Mid-infrared plasmonically induced absorption and transparency in a Si-based structure for temperature sensing and switching applications," *Optics Communications*, 2019, 430: 227–233.

[25] Y. Xie, Y. Ye, Y. Liu, S. Wang, J. Zhang, and Y. Liu, "Synchronous slow and fast light based on plasmon-induced transparency and absorption in dual hexagonal ring resonators," *IEEE Transactions on Nanotechnology*, 2018, 17(3): 552–558.

[26] Q. Lin, X. Zhai, L. L. Wang, X. Luo, G. D. Liu, J. P. Liu, *et al.*, "A novel design of plasmon-induced absorption sensor," *Applied Physics Expres*s, 2016, 9(6): 062002.

[27] M. Bahramipanah, S. Dutta-Gupta, B. Abasahl, and O. J. F. Martin, "Cavity-coupled plasmonic device with enhanced sensitivity and figure-of-merit," *ACS Nano*, 2015, 9(7): 7621–7633.

[28] K. Wen, Y. Hu, L. Chen, J. Zhou, M. He, L. Lei, *et al.*, "Single and dual-plasmonic induced absorption in a subwavelength end-coupled composite-square cavity," *Applied Optics*, 2017, 56(30): 8372–8377.

[29] J. F. Hu, J. Liu, B. Liu, J. Chen, H. Q. Liang, and G. Q. Li, "Plasmon-induced absorption and its applications for fast light and sensing based on double-stub resonators," *Optik*, 2018, 159: 254–260.

[30] J. Nikolina and C. Norbert, "High-resolution plasmonic filter and refractive index sensor based on perturbed square cavity with slits and orthogonal feeding scheme," *Plasmonics*, 2018, 13: 1–6.